Coupled Rectangular Bars Between Parallel Plates*

WILLIAM J. GETSINGER†, MEMBER, IRE

Summary—Curves are presented giving the even-mode fringing capacitance, the odd-mode fringing capacitance, and the difference between odd- and even-mode fringing capacitances for wide ranges of thickness and spacing of rectangular bars centered between parallel plates. Simple formulas are given relating these capacitances to even- and odd-mode characteristic impedances of coupled rectangular bars. Possible applications to strip-line and other circuits are described.

The Appendix gives the derivation of the fringing capacitances by conformal mapping techniques. The results are exact for bars extending in width infinitely far from the coupling region, and have only small error (less than 1.24 per cent) for bars whose width is greater than about 35 per cent of the difference between plate spacing and bar thickness.

I. General

IN WORKING with shielded strip-line, it is sometimes desirable to couple center conductors having appreciable thickness. The cross section of a typical structure of this type is shown in Fig. 1. There are two parallel ground planes spaced a distance b apart, and two rectangular bars located parallel to, and midway between, the ground planes. It is well known[1,2] that TEM propagation along such a structure can be described in terms of two orthogonal modes, usually denoted as the even mode and the odd mode. In the even mode, both center conductors are at the same potential, while in the odd mode, the two center conductors are at opposite potentials with respect to the ground planes. These two TEM modes have different characteristic impedances, which are intimately related to the static capacitances of the bars to ground. These capacitances are designated conventionally as parallel-plate capacitances between bar and ground planes, and fringing capacitances from ends and corners of the bars, as indicated schematically in Fig. 1.

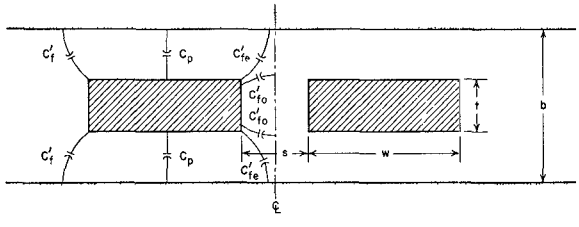

Fig. 1—Coupled rectangular bars centered between parallel plates.

Cohn[3] has previously considered coupled rectangular bars between parallel plates. He gives rigorous results, based on a conformal mapping solution, for the zero-thickness case, and adds correction terms to the zero-thickness case to obtain approximate results for bars of finite thickness. In a later paper,[4] Cohn provides an improved approximation for the odd-mode correction term. Horgan[5] has approached the problem by dividing the cross section of the coupled rectangular bar structure into insulated rectangular boxes, for each of which potential solutions were available. Horgan then corrected these approximations by adding new potential functions such that total potentials were matched across the insulating bounds, and the resulting capacitance was a maximum. Horgan's results, like those of Cohn, were written as exact thin-strip capacitance solutions plus correction terms.

The present paper, however, does not modify a solution for coupled thin strips, but determines the fringing capacitances for bars extending in width infinitely far from the coupling region by an exact conformal mapping method, and presents these fringing capacitances directly on graphs for wide ranges of bar thickness and spacing. The use of accurate graphs, giving the fringing capacitances directly, allows the total capacitance (and thus characteristic impedance, or alternatively, bar width) of any of a variety of structures to be determined quite easily by simply summing the appropriate fringing and parallel plate capacitances, as will be shown subsequently.

II. Technical Description

The characteristic impedance Z_0 of a lossless uniform transmission line operating in the TEM mode is related to its shunt capacitance by

$$Z_0\sqrt{\epsilon_r} = \frac{\eta}{(C/\epsilon)} \text{ ohms} \qquad (1)$$

where

$\sqrt{\epsilon_r}$ = the relative dielectric constant of the medium in which the wave travels

η = the impedance of free space = 376.7 ohms per square

* Received by PGMTT, August 23, 1961; revised manuscript received, October 4, 1961. This work was supported by the U. S. Army Signal Res. and Dev. Lab., Fort Monmouth, N. J., as part of Contract DA-36-039 SC-87398.

† Stanford Research Institute, Menlo Park, Calif.

[1] B. M. Oliver, "Directional electromagnetic couplers," PROC IRE, vol. 42, pp. 1686–1692; November, 1954.

[2] E. M. T. Jones and J. T. Bolljahn, "Coupled-strip-transmission-line filters and directional couplers," IRE TRANS. ON MICROWAVE THEORY AND TECHNIQUES, vol. MTT-4, pp. 75–81; April, 1956.

[3] S. B. Cohn, "Shielded coupled-strip transmission line," IRE TRANS. ON MICROWAVE THEORY AND TECHNIQUES, vol. MTT-8, pp. 29–38; October, 1955.

[4] S. B. Cohn, "Thickness corrections for capacitive obstacles and strip conductors," IRE TRANS. ON MICROWAVE THEORY AND TECHNIQUES, vol. MTT-8, pp. 638–644; November, 1960.

[5] J. D. Horgan, "Coupled strip transmission lines with rectangular inner conductors," IRE TRANS. ON MICROWAVE THEORY AND TECHNIQUES, vol. MTT-5, pp. 92–99; April, 1957.

C/ϵ = the ratio of the static capacitance per unit length between conductors to the permittivity (in the same units) of the dielectric medium (this ratio is independent of the dielectric constant).

The even- and odd-mode impedances of coupled TEM lines[1,2] can be found by substituting even- and odd-mode capacitances of the lines in (1).

A generalized schematic diagram of shielded coupled-strip transmission line is shown in Fig. 2. The circles represent the coupled conductors. The capacitance to ground for a single conductor, when both conductors are at the same potential, is C_{oe}, the even-mode capacitance. The capacitance to ground when the two conductors are oppositely charged with respect to ground is C_{oo}, the odd-mode capacitance.

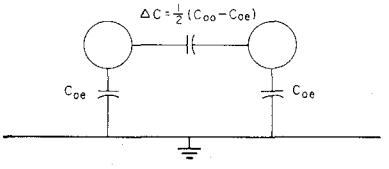

Fig. 2—Generalized schematic diagram.

The structure of Fig. 1 is composed of parallel-planar surfaces. This makes it practical to consider the total capacitance of a given strip to be composed of parallel-plane capacitances plus appropriate fringing capacitances. (Fringing capacitances take into account the distortion of the field lines in the vicinity of the edges of the plane strips.) Fig. 1 relates the various capacitances to the geometry of the structure under consideration. Thus, it can be seen that the total even-mode capacitance C_{oe}/ϵ from one bar to ground is

$$C_{oe}/\epsilon = 2(C_p/\epsilon + C_{fe}'/\epsilon + C_f'/\epsilon) \quad (2)$$

and the total odd-mode capacitance C_{oo}/ϵ from one bar to ground is

$$C_{oo}/\epsilon = 2(C_p/\epsilon + C_{fo}'/\epsilon + C_f'/\epsilon). \quad (3)$$

In (2) and (3), C_p is the parallel-plate capacitance from the top or bottom side of one bar to the nearest ground plane; C_{fe}' is the capacitance to ground from one corner and half the associated vertical wall in the coupling region of a bar for even-mode excitation; C_{fo}' is the capacitance to ground from one corner and half the associated vertical wall in the coupling region of a bar for odd-mode excitation; and C_f' is the capacitance to ground from one corner and half the associated vertical wall away from the coupling region of a bar for any

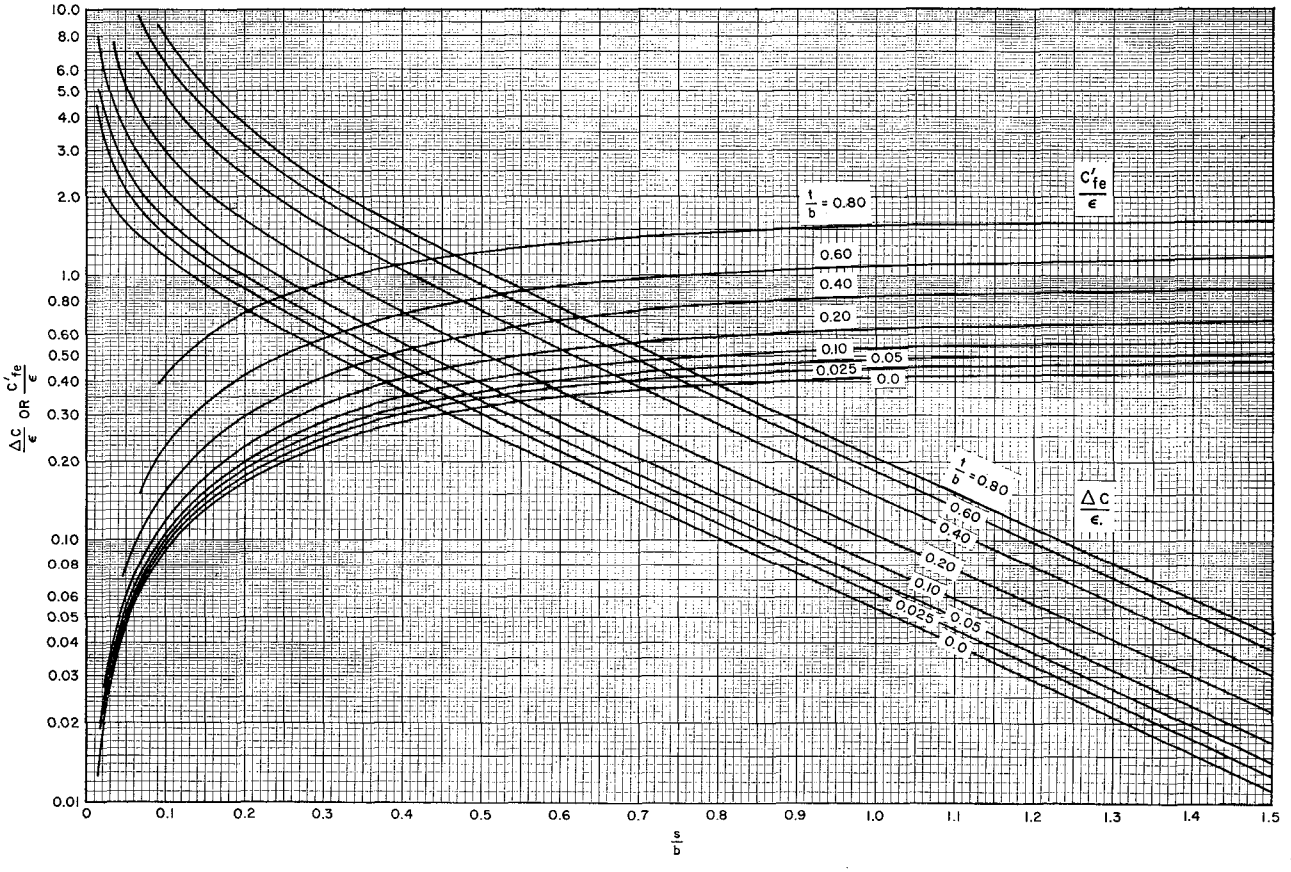

Fig. 3—Fringing capacitances for coupled rectangular bars.

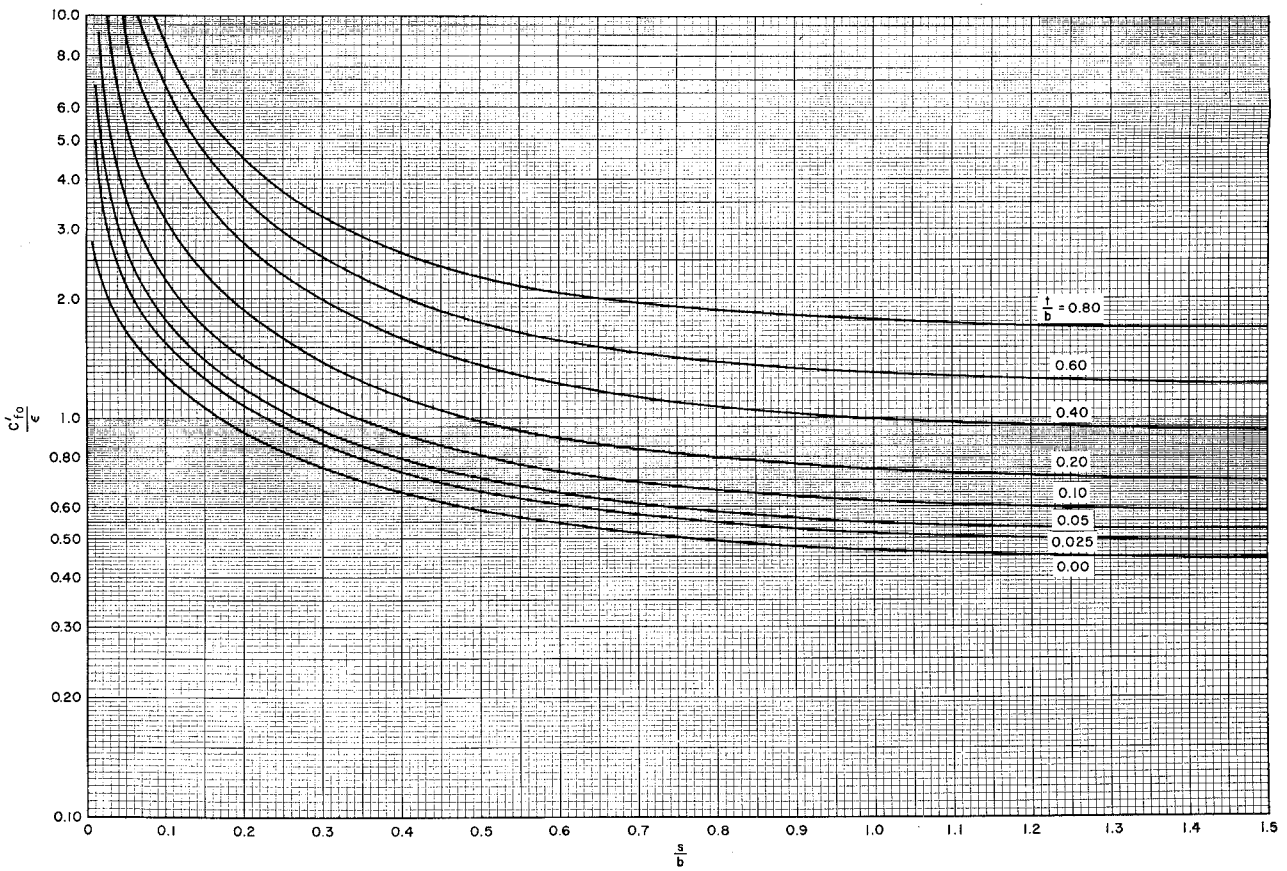

Fig. 4—Odd-mode fringing capacitance for coupled rectangular bars.

excitation. Consideration of Fig. 2 and the definitions of even- and odd-mode capacitances show that the capacitance, $\Delta C/\epsilon$, from one bar to the other is given by

$$\Delta C/\epsilon = \tfrac{1}{2}(C_{oo}/\epsilon - C_{oe}/\epsilon). \tag{4}$$

Subtraction of (2) from (3) shows that $\Delta C/\epsilon$ can be written entirely in terms of the fringing capacitances as

$$\Delta C/\epsilon = C_{fo}'/\epsilon - C_{fe}'/\epsilon. \tag{5}$$

Fig. 3 is a plot of both even-mode fringing capacitances, C_{fe}'/ϵ, and the capacitance, $\Delta C/\epsilon$, between bars as functions of bar thickness and spacing, while Fig. 4 is a similar graph for the odd-mode fringing capacitance, C_{fo}'/ϵ. The derivation of Figs. 3 and 4 is described in the Appendix. Fig. 5 gives the fringing capacitance C_f'/ϵ from the outer edges of the bars as a function of thickness. The parallel plate capacitance C_p/ϵ is given by

$$C_p/\epsilon = 2\,\frac{w/b}{1 - t/b}, \tag{6}$$

where w and t are the width and thickness of the bar. Through the use of the above relations and figures, it is possible to relate physical dimensions of the given configuration to even- and odd-mode capacitances or impedances.

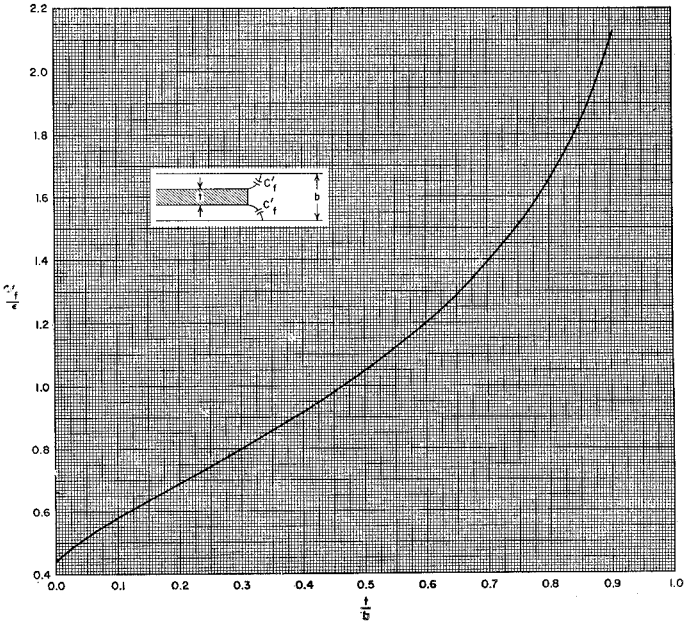

Fig. 5—Fringing capacitance for an isolated rectangular bar.

III. Use of the Graphs

Usually, an engineer designing parallel-coupled lines first determines the values of even- and odd-mode impedances, Z_{oe} and Z_{oo}, or even- and odd-mode capacitances, C_{oe} and C_{oo}, as required by theoretical considerations. He then wishes to determine the corresponding physical line dimensions. A simple procedure accomplishes this. Using (1) in (4) gives

$$\Delta C/\epsilon = \frac{\eta}{2\sqrt{\epsilon_r}}\left(\frac{1}{Z_{oo}} - \frac{1}{Z_{oe}}\right). \tag{7}$$

Values of b and t are selected and used with the value of $\Delta C/\epsilon$ found from (7) to determine s/b directly from Fig. 3. Next, C_{oe}/ϵ is determined by using Z_{oe} in (1), and then C_{fe}'/ϵ and C_f'/ϵ are found from t/b and from the graphs of Figs. 3 and 5. These quantities can be substituted into the following equation to give w/b

$$w/b = \frac{1}{2}\left(1 - \frac{t}{b}\right)\left(\frac{C_{oe}/\epsilon}{2} - C_{fe}'/\epsilon - C_f'/\epsilon\right). \tag{8}$$

Eq. (8) results from substitution of (6) in (2), and rearrangement of terms.

Thus, the two unknown dimensions, s/b and q/b, have been determined.

IV. Considerations of Accuracy

If the bar width w is allowed to become too small, there is interaction of the fringing fields from the two edges, and the decomposition of total capacitance into parallel plane capacitance and fringing capacitances (which are based on infinite bar widths) is no longer accurate. Cohn[6] shows that for a single bar centered between parallel planes, the error in total capacitance from interaction of the fringing fields is about 1.24 per cent for $w/(b-t)=0.35$, where w is the width of the bar, t is its thickness, and b is again the ground-plane spacing. If a maximum error in total capacitance of approximately this magnitude is allowed, then it is necessary that $[(w/b)/(1-t/b)]>0.35$.

Should this inequality be too restricting, it is possible to make approximate corrections based on an increase in the parallel-plate capacitance, to compensate for the loss of fringing capacitance due to interaction of fringing fields. If an initial value w_1/b is found to be less than $0.35[1-(t/b)]$, a new value, w_2/b can be used, where

$$w_2/b = \{0.07[1 - (t/b)] + w_1/b\}/1.20 \tag{9}$$

provided that $0.1<(w_2/b)/[1-(t/b)]<0.35$. This formula is based on a linear approximation to the exact fringing capacitance of single thin strip for a $(w/b)/[1-(t/b)]$ ratio between 0.1 and 0.35. As the relative strip width becomes narrower than 0.35, the fringing capacitance, defined as total capacitance less parallel plate capacitance, becomes smaller. The total capacitance is given by substituting into (1) the exact thin-strip formula for Z_o given by Cohn.[6] Eq. (9) adds sufficient parallel-plate capacitance to compensate for the loss of fringing capacitance. The loss of fringing is assumed to vary linearly below a relative width of 0.35. Although the formula is analytically only approximate, it is sufficiently accurate for practical use because it does no more than give a small correction to a quantity that is reasonably close to the exact value. It can be used with both isolated and coupled bars.

The derivations for the fringing capacitances are exact for bars extending in width infinitely far to the right and left, away from the coupling region. The original computed values were accurate to eight places. However, in order to give values of fringing capacitance associated with constant t/b, it was necessary to use graphical interpolation, as pointed out in the Appendix. The plotted points were held to an accuracy of three figures after the decimal point, so that the interpolated results are slightly less accurate. The curves of Figs. 3 and 4 are accurate to within about one or two per cent. However, since fringing capacitances are usually not the predominant part of the total capacitance of a structure, total capacitance can be specified with somewhat greater accuracy.

Fig. 5, for the fringing capacitance C_f'/ϵ of a single bar extending infinitely far in one direction, is based on an exact solution given by Cohn.[6] The same data can be found from Figs. 3 and 4 by reading either C_{fe}'/ϵ or C_{fo}'/ϵ as functions of t/b for large s/b. The accuracy of Fig. 5 is thus limited by the precision to which the graph can be read.

V. Applications

Figs. 3–5, for fringing capacitances, can be used for a variety of structures, as shown in Fig. 6, simply by adding the appropriate fringing capacitances with the parallel plate capacitances to give the even-mode capacitance, the odd-mode capacitance, or the total capacitance. Use of (1) then gives the associated characteristic impedance. Thus, Fig. 6(a) shows ordinary shielded strip-line and the capacitances involved when it is open, closed at one end, or closed at both ends.[7] The structure closed at one end is sometimes called trough-line, the structure closed at both ends is sometimes called rectangular coaxial line. Similarly, the even- and odd-mode capacitances and impedances can be determined for the coupled structures shown in Fig. 6(b) for open or closed ends. This simple technique may also be applicable when the arms of an N-way power divider in shielded strip-line must run parallel for some distance, as shown in plan in Fig. 6(c). The even-mode fringing

[6] S. B. Cohn, "Problems in strip transmission lines," IRE Trans. on Microwave Theory and Techniques, vol. MTT-3, pp. 119–126; March, 1955.

[7] The notation in Fig. 6(a), $C_{fo}'(s_a/b)$ and $C_{fo}'(s_b/b)$, does not indicate multiplication, but merely that C_{fo}' is to be evaluated at s_a/b or s_b/b, as appropriate for the spacing from the nearby wall.

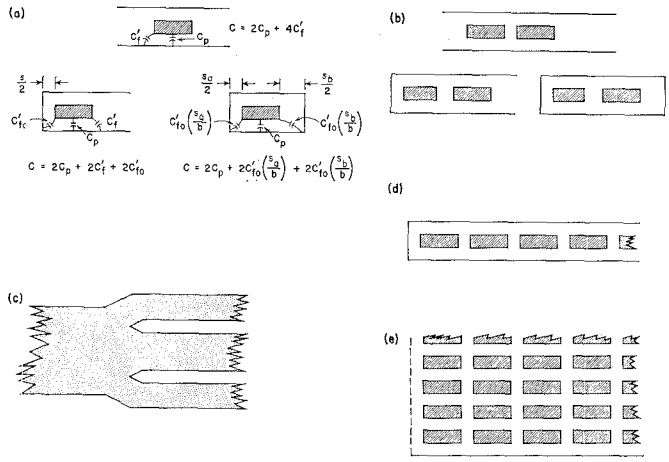

Fig. 6—Possible applications.

capacitance C_{fe}' would then be appropriate for adjacent edges of the arms.

Both even- and odd-mode fringing capacitances would be necessary for multi-element lines, such as are shown in Fig. 6(d) and (e). The cross section shown in (d) could be part of a meander or interdigital line, while that in (e) might be part of a finite or infinite array of elements, which might be used as an artificial dielectric medium.

The curves given herein can be used in the design of wide-band, parallel-coupled, strip-transmission-line filters, such as described by Matthaei.[8] Also, Bolljahn and Matthaei[9] have presented design data for slow-wave structures and filters using parallel-coupled arrays of line elements. Some realizations of those devices use relatively wide rectangular bars to form an interdigital line, comb line, meander line, or similar slow-wave line. In such cases, the curves given herein greatly facilitate the process of precision design.

Coupled rectangular bars may also be applied to strip-line directional couplers, described by Jones and Bolljahn,[2] in which the use of rectangular bars allows closer coupling to be achieved with less critical tolerances.

Appendix

Derivation of Fringing Capacitances

Preliminary

It is desired to determine the static fringing capacitances shown on the structure of Fig. 1 by means of conformal mapping techniques.[10,11] This can be done by subjecting the boundaries of the structure to transformations under which capacitance is invariant, and that lead to a new structure for which capacitance is known. Subtraction of parallel plate capacitances of the original structure from the total capacitance then leaves the fringing capacitances. The analysis will be limited to structures in which the bars are so wide that interaction between fringing fields of the two edges of a single bar is negligible. As discussed in Section IV, this requires that the approximate relation $\{(w/b)/[1-(t/b)]\}>0.35$ be held. Under these conditions it is possible to let the bars extend in width infinitely far to the left and right, without disturbing the fringing fields appreciably in the coupling region where the capacitances interact. The vertical centerline shown on Fig. 1 may be replaced by an electric wall (conductor) for the odd mode, or by a magnetic wall for the even mode, in consideration of the symmetry of the structure. Also, the electric field can lie parallel to the horizontal centerline where no conductor exists, but cannot cross it because of the symmetry. Therefore, a magnetic wall can be placed along the horizontal centerline. These modifications allow analysis of only one-quarter of the total symmetrical structure. The mathematical model is shown on the z-plane in Fig. 7. Conductors are indicated by solid lines and magnetic walls by broken lines. The upper-case letters denote pertinent points of the structure and will serve as references when transformations to different complex planes are made.

The analysis essentially consists in transformation of the contours of the structure on the z-plane into a parallel-plate representation on another complex plane, where capacitance can be computed directly.

The static electric fields of interest lie within the polygon defined by the boundaries of the structure on the z-plane. The interior of this polygon is to be mapped onto the first quadrant of the t-plane shown in Fig. 7. The integral resulting from direct use of the Schwarz-Christoffel transformation is

$$z = \int \frac{(1-t^2)^{1/2}}{(1-k^2t^2)^{1/2}(1-k^2t^2\,\mathrm{sn}^2\,a)}\,dt, \qquad (10)$$

where, for the present, $1/k$ and $1/(k\,\mathrm{sn}\,a)$ are the points on the real t axis to which the corner F and the point $-j_\infty$ map from the z-plane. This integral can be evaluated by further relating the first quadrant of the t-plane to the interior of the fundamental rectangle of Jacobian elliptic functions on the u-plane, also shown in Fig. 7, using the transformation

$$t = \mathrm{sn}\,u. \qquad (11)$$

This substitution gives

$$z = \int \frac{\mathrm{cn}^2\,u\,du}{1-k^2\,\mathrm{sn}^2\,u\,\mathrm{sn}^2\,a}. \qquad (12)$$

[8] G. L. Matthaei, "Design of wide-band (and narrow-band) band pass microwave filters on the insertion loss basis," IRE Trans. on Microwave Theory and Techniques, vol. MTT-8, pp. 580–593; November, 1960.

[9] J. T. Bolljahn and G. L. Matthaei, "Microwave Filters and Coupling Structures," Stanford Res. Inst., Menlo Park, Calif., Report No. 1, Contract DA 36-039 SC-87398; April, 1961.

[10] W. R. Smythe, "Static and Dynamic Electricity," McGraw-Hill Book Co., Inc., New York, N. Y.; 1939.

[11] E. Weber, "Electromagnetic fields: theory and applications," in "Mapping of Fields," John Wiley and Sons, Inc., New York, N. Y., vol. 1; 1950.

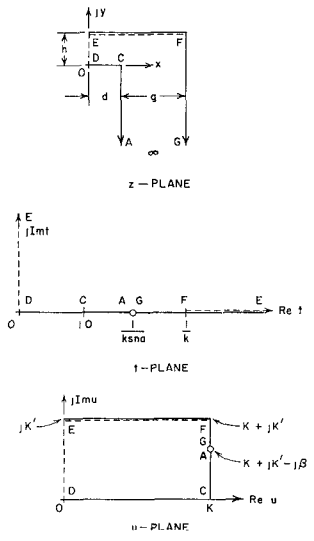

Fig. 7—Mathematical models on z-plane, t-plane, and u-plane.

In the above equations, sn u and cn u are Jacobian elliptic functions having a quarter period K determined by k, denoted by convention as the modulus. By virtue of (11), a can be considered to be a point on the perimeter of the fundamental rectangle on the u-plane. It is convenient to let

$$a \triangleq K - j\beta \tag{13}$$

by definition. Ultimately, k and β will be used as independent variables.

The mapping of the z-plane onto the t-plane in this manner has been carried through by Cockroft,[12] whose symbols are retained in Fig. 7 and in the equations given in this section. The distances on the z-plane are given by Cockroft as

$$d = K\left[1 - \frac{\text{dn } a}{k^2 \text{ sn } a \text{ cn } a} Z(a)\right] \tag{14}$$

$$g = -j\frac{\pi}{2}\frac{\text{dn } a}{k^2 \text{ sn } a \text{ cn } a} \tag{15}$$

$$h = jd\frac{K'}{K} - j\frac{\pi}{2}\frac{\text{dn } a}{k^2 \text{ sn } a \text{ cn } a}\left(\frac{a}{K} - 1\right). \tag{16}$$

It should be noted that g is a negative quantity and h an imaginary one. The quantity dn a is also a Jacobian elliptic function and $Z(a)$ is the Jacobian zeta-function. The quantity K' is the same function of the complementary modulus k', as K is of k. The moduli are related by

$$k^2 + k'^2 = 1. \tag{17}$$

[12] J. D. Cockroft, "The effect of curved boundaries on the distributions of electrical stress round conductors," *J. IEE*, vol. 66, pp. 385–409; April, 1926.

Comparison of Fig. 1 with Fig. 7 shows that the conventional normalized dimensions s/b and t/b of the rectangular bar structure are related to Cockroft's dimensions d, g, and h by

$$s/b = \frac{-jh}{d - g}$$

$$t/b = \frac{d}{d - g}. \tag{18}$$

Thus, the physical dimensions of the structure of Fig. 1 have been related to the parameters of the u-plane by (14)–(16) and (18).

Now it is necessary to transform the t-plane to a parallel-plate structure, and determine fringing capacitances as functions of u-plane parameters.

Odd-Mode Capacitance

The two rectangular bars in Fig. 1 are at equal and opposite voltages when energized in the odd mode, so that the plane midway between the bars is at zero potential. Thus, a conductor may be placed in this plane without disturbing the fields. This is indicated by the solid line between E and F on the planes of Fig. 7. For this condition, the t-plane configuration can be transformed to a parallel-plate structure of unit height by the function

$$w = \frac{1}{\pi}\ln\left(\frac{1 + tk \text{ sn } a}{1 - tk \text{ sn } a}\right), \tag{19}$$

which moves the singularity at AG to infinity. The interesting region of the w-plane is shown in Fig. 8.

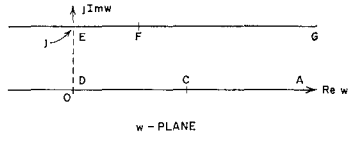

Fig. 8—w-plane for odd-mode capacitance.

The fringing capacitance is the difference between the total capacitance of the structure (total capacitance is the same on both z- and w-planes) and the parallel-plane capacitance of the z-plane structure. A reasonable definition for z-plane parallel-plate capacitance C_{pz} is parallel-plate capacitance existing between the ground plane and the full length of the rectangular bar. Mathematically,

$$\frac{C_{pz}}{\epsilon} = \lim_{z \to -j\infty} \text{Im } (z/g). \tag{20}$$

Then the odd-mode fringing capacitance C_{fo}'/ϵ is

$$C_{fo}'/\epsilon = \lim_{z \to -j\infty} [w(z) - \text{Im } (z/g)] \tag{21}$$

where $w(z)$ is given by (19) related to the z-plane. In order to evaluate C_{fo}'/ϵ, it is necessary that both w and Im(z/g) be expressed as functions of u. The limit must

also be in terms of u. From Fig. 7 it can be seen that as $z \to -j_\infty$ along the path from C to A, then $u \to K + jK' - j\beta$ along the path from C to A. Thus

$$C_{fo}'/\epsilon = \lim_{u \to K + jK' - j\beta} \left[w(u) - \operatorname{Im} \frac{z(u)}{g} \right]. \tag{22}$$

Substitution of (11) in (19) gives

$$w(u) = \frac{1}{\pi} \ln \left(\frac{1 + k \operatorname{sn} a \operatorname{sn} u}{1 - k \operatorname{sn} a \operatorname{sn} u} \right). \tag{23}$$

The limiting process is simplified by letting

$$u = K + jK' - j\beta - j\delta \tag{24}$$

where $\delta \to 0$ as $u \to K + jK' - j\beta$ along the path from C to A. Assuming very small δ, and using various elliptic function equivalences, such as may be found in Byrd and Friedman,[13] (23) reduces to

$$\underset{\delta \to 0}{w(u)} = \frac{1}{\pi} \ln 2 - \frac{1}{\pi} \ln \left(-j \frac{\operatorname{cn} a \operatorname{dn} a}{\operatorname{sn} a} \right) - \frac{1}{\pi} \ln \delta. \tag{25}$$

Cockroft's[12] (44) gives $z(\delta)$ as

$$z(\delta) = (K + jK' - j\beta) \left[1 - \frac{\operatorname{dn} a}{k^2 \operatorname{sn} a \operatorname{cn} a} Z(a) \right] - \frac{1}{2} \frac{\operatorname{dn} a}{k^2 \operatorname{sn} a \operatorname{cn} a} \ln \frac{\Theta(jK' - j\delta)}{\Theta(2K + jK' - 2j\beta)}. \tag{26}$$

Using (26) with (15), and passing to the limit of δ approaching zero, gives

$$\operatorname*{Im}_{\delta \to 0} \left[\frac{z(u)}{g} \right] = (K' - \beta) \left[\frac{1}{g} - \frac{2j}{\pi} Z(a) \right] - \frac{K'}{4K} - \frac{1}{2\pi} \ln \frac{2kk'K}{\pi} - \frac{1}{\pi} \ln \delta. \tag{27}$$

In (26) and (27) the term Θ is Jacobi's theta function.[14] Now (25) and (27) can be substituted into (22), yielding

$$C_{fo}'/\epsilon = \frac{1}{\pi} \ln \frac{2j \operatorname{sn} a}{\operatorname{cn} a \operatorname{dn} a} + \frac{1}{2\pi} \ln \frac{2kk'K}{\pi} + \frac{K'}{2K} + (K' - \beta) \left[\frac{2j}{\pi} Z(a) - \frac{1}{g} \right] - \frac{1}{\pi} \ln \Theta(jK' - 2j\beta). \tag{28}$$

This is the final form in which odd-mode fringing capacitance will be presented.

[13] P. F. Byrd and M. D. Friedman, "Handbook of Elliptic Integrals for Physicists and Engineers," Springer-Verlag, Berlin, Germany; 1954.

[14] E. T. Copson, "Theory of Functions of a Complex Variable," Oxford University Press, London; pp. 405–407; 1960.

Even-Mode Capacitance

The two rectangular bars in Fig. 1 are at the same potential when energized in the even mode, so that no electric field crosses the plane midway between them. Thus, a magnetic wall may be placed in this plane without disturbing the fields. This is indicated by the broken line between E and F on the planes of Fig. 7. The upper half of the t-plane is mapped into a strip of unit height on a t_1-plane in such a manner that the singularity at AG is removed to infinity by the transformation

$$t_1 = \frac{1}{\pi} \ln \left[\frac{tk \operatorname{sn} a + 1}{tk \operatorname{sn} a - 1} \right]. \tag{29}$$

The t_1-plane is shown in Fig. 9. Notice that the upper half of the t-plane maps into the strip directly below the Re t_1 axis. The positive half of this strip is next mapped onto the lower half of a t_2-plane, shown in Fig. 9 by the transformation

$$t_2 = M - 1 + M \cosh \pi t_1, \tag{30}$$

where

$$M \triangleq \frac{2}{1 + \cosh \pi t_1(F)} = -\frac{\operatorname{cn}^2 a}{\operatorname{sn}^2 a}. \tag{31}$$

Finally, the desired parallel-plate configuration is achieved by mapping the lower half of the t_2-plane onto the positive half of a strip of unit height on the w_1-plane, using the transformation

$$w_1 = \frac{1}{\pi} \operatorname{arc\,cosh} (-t_2). \tag{32}$$

The w_1-plane is also shown on Fig. 9. Combining (11), (29), (30), (31), and (32) gives w_1 as a function of u

$$w_1(u) = \frac{1}{\pi} \operatorname{arc\,cosh} \left\{ 1 + \frac{cn^2 a}{\operatorname{sn}^2 a} + \frac{\operatorname{cn}^2 a}{\operatorname{sn}^2 a} \cdot \left[\frac{(k \operatorname{sn} a \operatorname{sn} u)^2 + 1}{(k \operatorname{sn} a \operatorname{sn} u)^2 - 1} \right] \right\}. \tag{33}$$

As with the odd mode, it is convenient to use the variable δ, defined by (24), in passing to the limit. When (24) is substituted in (33) and appropriate approximations made for small δ, manipulation yields

$$\underset{\delta \to 0}{w_1(u)} = \frac{1}{\pi} \ln 2 + \frac{1}{\pi} \ln \left(-j \frac{\operatorname{cn} a}{\operatorname{sn} a \operatorname{dn} a} \right) - \frac{1}{\pi} \ln \delta. \tag{34}$$

Using the definition of z-plane parallel-plate capacitance given in (20), the even-mode fringing capacitance, C_{fe}'/ϵ is

$$\frac{C_{fe}'}{\epsilon} = \lim_{\delta \to 0} \left[w_1(u) - \operatorname{Im} \frac{z(u)}{g} \right]. \tag{35}$$

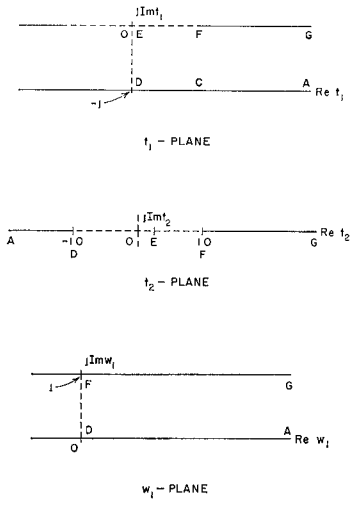

Fig. 9—t_1-plane, t_2-plane, and w_1-plane for even-mode capacitance.

Substitution of (34) and (27) in (35) yields, after simplification,

$$\frac{C_{fe}'}{\epsilon} = \frac{1}{\pi}\ln\left(\frac{-2j\ \mathrm{cn}\ a}{\mathrm{sn}\ a\ \mathrm{dn}\ a}\right) + \frac{1}{2\pi}\ln\frac{2kk'K}{\pi} + \frac{K'}{4K} + (K'-\beta)\left[\frac{2jZ(a)}{\pi} - \frac{1}{g}\right] - \frac{1}{\pi}\ln\Theta(jK' - 2j\beta). \tag{36}$$

This is the final form in which the even-mode fringing capacitance will be given.

Difference of Fringing Capacitances

The difference between fringing capacitances, $C_{fo}'/\epsilon - C_{fe}'/\epsilon$, is a very useful quantity because in most coupled structures it is also half of the difference between total odd-mode and even-mode capacitances. This difference is found by subtracting (36) from (28), yielding

$$\frac{C_{fo}}{\epsilon} - \frac{C_{fe}'}{\epsilon} = \frac{1}{\pi}\ln\left(-\frac{\mathrm{sn}^2\ a}{\mathrm{cn}^2\ a}\right). \tag{37}$$

Evaluation of Formulas

The curves of C_{fe}'/ϵ and $C_{fo}'/\epsilon - C_{fe}'/\epsilon$ as functions of s/b and t/b were determined in the following manner: values of $0<k<1$ were selected from tables[13,15] that determined K, K', and k'; then for each value of k, a range of values of β/K' was selected from tables[15] that gave sn (β, k'), cn (β, k'), and dn (β, k'). These functions are related to sn a, cn a, and dn a by

$$\mathrm{sn}\ (a, k) = \frac{1}{\mathrm{dn}\ (\beta, k')},$$
$$\mathrm{cn}\ (a, k) = jk'\frac{\mathrm{sn}\ (\beta, k')}{\mathrm{dn}\ (\beta, k')},$$
$$\mathrm{dn}\ (a, k) = k'\frac{\mathrm{cn}\ (\beta, k')}{\mathrm{dn}\ (\beta, k')}. \tag{38}$$

The zeta function can be expressed as

$$Z(a, k) = j\left[Z(\beta, k') + \frac{\pi\beta}{2KK'} - k'^2\frac{\mathrm{sn}\ (\beta, k')\ \mathrm{cn}\ (\beta, k')}{\mathrm{dn}\ (\beta, k')}\right], \tag{39}$$

where

$$Z(\beta, k') = \frac{\Theta'(\beta, k')}{\Theta(\beta, k')}. \tag{40}$$

The theta functions were evaluated using a Fourier series expansion.[14] Values of t/b, s/b, C_{fe}'/ϵ and $C_{fo}'/\epsilon - C_{fe}'/\epsilon$ were then calculated from (18), (26), and (37), and plotted as function of β/K', with k as parameter. Values of t/b were selected to be used as parameters on and final graph, and the related values of k and β/K' were taken from the t/b graph and tabulated. The values of k and β/K' at each point were used to determine related values of s/b, C_{fe}'/ϵ, and $C_{fo}'/\epsilon - C_{fe}'/\epsilon$ from their graphs. In this way it was possible to compile values of s/b, C_{fe}'/ϵ and $C_{fo}'/\epsilon - C_{fe}'/\epsilon$ for constant t/b. This compilation was used to plot the final sets of curves shown in Figs. 3 and 4.

[15] G. W. Spenceley and R. M. Spenceley, "Smithsonian Elliptic Functions Tables," Smithsonian Misc. Coll., Washington, D. C., vol. 109; 1947.